J Mater Sci (2008) 43:5336–5341
DOI 10.1007/s10853-008-2779-7

Hydrogen sorption characteristics of the composites 90 wt.% Mg (MgH_2)–10 wt.% $V_{0.855}Ti_{0.095}Fe_{0.05}$

Eli Grigorova · Mitko Khristov · Maria Khrussanova · Pavel Peshev

Received: 27 February 2008 / Accepted: 4 June 2008 / Published online: 24 June 2008

Abstract The hydrogen absorption–desorption characteristics of composites containing 90 wt.% Mg or MgH_2 and 10 wt.% of the intermetallic compound $V_{0.855}Ti_{0.095}Fe_{0.05}$ obtained by mechanical alloying for 1 and 5 h in an inert medium were investigated. Absorption measurements were performed under a hydrogen pressure $P = 1$ MPa at temperatures of 623, 573, 523, and 473 K. Dehydriding was studied at 623 and 573 K and a pressure of 0.15 MPa. It was established that the presence of the additive improved significantly the hydriding kinetics of magnesium while the effect of the duration of mechanical alloying was less pronounced. Due to the small difference in specific surface areas and crystallite sizes, both composites investigated showed no substantial difference in behavior during absorption and desorption of hydrogen. The best absorption–desorption properties were found with the composite 90 wt.% Mg–10 wt.% $V_{0.855}Ti_{0.095}Fe_{0.05}$ mechanically activated for 5 h.

Introduction

Magnesium and magnesium-based materials are promising for hydrogen storage and have for this reason been the subject of many investigations. Elemental magnesium has a high hydrogen absorption capacity and a low cost but is difficult to activate and its full capacity is only attained at high temperatures. That is why efforts have been made to obtain materials based on magnesium, which would preserve its high absorption capacity, reaching suitable sorption characteristics under milder hydriding–dehydriding conditions. With view to improving the hydrogen exchange kinetics, a large number of studies were performed during the past years on composites of magnesium with different additives, obtained by high-energy ball milling in an inert or reactive medium. A favorable effect was found with addition of some metals [1–13], metal oxides [14–23], binary and ternary intermetallics [24–40], inorganic salts [41], and graphite [42–45]. Recently, starting with a study by Schulz's research group in Canada [46], magnesium hydride, MgH_2, instead of magnesium, was often used with the same kinds of additives in composite preparation. This is due, above all, to the fact that MgH_2 is brittle and during grinding larger surface area materials having no tendency to agglomerate are expected to be obtained. Exhaustive reviews on the MgH_2-based composites are given in recent papers of the Canadian and the GKSS-Forschungszentrum group in Germany [46–49]. Thus, the mechanical activation of the mixture MgH_2–5 at.% V leads to the formation of a nanocomposite containing $\beta MgH_2 + \gamma MgH_2 + VH_{0.81}$ which desorbs hydrogen for 25 min at 523 K [46]. It is found that a decrease in particle size and a more defective structure with a larger specific surface area are achieved after prolonged milling of MgH_2 with an Nb_2O_5 additive, which plays the role of a dispersing agent [48]. Dolci et al. [23] have investigated the effect of Nb_2O_5 on the hydriding/dehydriding properties of the MgH_2-based system and illustrated that the oxide has been partially reduced by H_2. They suggest that it plays an active chemical role during absorption/desorption processes. It is known, however, that prolonged grinding in a high-energy mill results in sticking of the particles and formation of agglomerates. That is why both the character of the additive and the conditions of mechanical activation are

E. Grigorova (✉) · M. Khristov · M. Khrussanova · P. Peshev
Institute of General and Inorganic Chemistry, Bulgarian Academy of Sciences, Acad. G. Bonchev Str., Building 11, Sofia 1113, Bulgaria
e-mail: egeorg@svr.igic.bas.bg

especially important for obtaining materials with appropriate properties for hydrogen storage.

As part of a large study on magnesium-based materials for hydrogen storage, this article deals with the hydrogen absorption–desorption characteristics of nanocomposites of the type 90 wt.% Mg (MgH_2)–10 wt.% $V_{0.855}Ti_{0.095}Fe_{0.05}$ obtained by mechanical activation in an inert medium. On the basis of previous results on magnesium composites containing the three 3d-elements [4] and on the hydrogen absorption–desorption properties of the alloy $V_{0.855}Ti_{0.095}Fe_{0.05}$ [50], this intermetallic phase is expected to have a positive effect on the magnesium behavior in the composites during hydriding and dehydriding.

Experimental

Powder magnesium of 99.9% purity was used for the preparation of the composites 90 wt.% Mg (MgH_2)–10 wt.% $V_{0.855}Ti_{0.095}Fe_{0.05}$ and of magnesium hydride. The synthesis of magnesium hydride proceeded at 623 K and a hydrogen pressure of 1.2 MPa. The alloy $V_{0.855}Ti_{0.095}Fe_{0.05}$, which will further on be denoted as VTiFe, was prepared from the corresponding metals by melting in an induction furnace under argon followed by annealing at 1273 K for 64 h in the same atmosphere. Before being added to magnesium or magnesium hydride, the alloy obtained was ground for 6 h in a Fritsch Pulverisette 6 planetary ball mill using stainless steel balls (diameter = 10 mm) with a rotation speed of 300 rpm and an alloy-to-balls ratio of 1:20.

The composites Mg-VTiFe and MgH_2-VTiFe were prepared by mechanical alloying in the same mill under argon at the following conditions: 1 or 5 h activation, sample-to-ball weight ratio of 1:10 and a rotation speed of 200 rpm.

The phase composition of the magnesium hydride obtained and of the hydrided and dehydrided composites was controlled by X-ray diffraction using CuKα radiation.

The absorption–desorption characteristics of the composites were determined by the volumetric method described in Ref. [51]. Hydriding was studied at 623, 573, 523, and 473 K and a pressure of 1 MPa, and dehydriding, at 623 and 573 K and a pressure of 0.15 MPa.

The specific surface area of the initial and hydrided composites was determined by low-temperatures nitrogen adsorption using the BET method. The crystallite sizes were calculated according to the Scherrer formula and the quantitative analysis of synthesized MgH_2 was made by using the Topas V3 programme [52].

The transfer from ball milling vial to the device for measuring the absorption/desorption properties and X-ray diffraction analyses of the samples were carried out in air.

Results and discussion

The X-ray diffraction patterns of (a) 90 wt.% Mg–10 wt.% $V_{0.855}Ti_{0.095}Fe_{0.05}$ ball milled 1 h, (b) 90 wt.% Mg–10 wt.% $V_{0.855}Ti_{0.095}Fe_{0.05}$ ball milled 5 h, (c) synthesized MgH_2, (d) 90 wt.% MgH_2–10 wt.% $V_{0.855}Ti_{0.095}Fe_{0.05}$ ball milled 1 h, and (e) 90 wt.% MgH_2–10 wt.% $V_{0.855}Ti_{0.095}Fe_{0.05}$ ball milled 5 h are shown in Fig. 1. It is evident that in the synthesized MgH_2 the main phase of MgH_2 is accompanied by magnesium oxide and traces of unreacted magnesium. From Fig. 1 it may be concluded that there are no substantial differences between the X-ray diffraction patterns of the composites ball milled for 1 and 5 h. According to Liang et al. [46] after intensive ball milling of MgH_2–5 at.% V, metastable orthorhombic γ-MgH_2 can be formed and MgH_2 can be reduced by vanadium, $VH_{0.81}$ phase appearing. After ball milling of 90 wt.% MgH_2–10 wt.% $V_{0.855}Ti_{0.095}Fe_{0.05}$, there is no formation of γ-MgH_2 and $VH_{0.81}$ phases.

The best absorption/desorption kinetics of the composites 90 wt.% Mg (MgH_2)–10 wt.% $V_{0.855}Ti_{0.095}Fe_{0.05}$ at different temperatures are shown in Figs. 2, 3, 5, and 6. The kinetic curves of hydriding at different temperatures of the composites Mg-VTiFe and MgH_2-VTiFe are presented in Figs. 2 and 3. Irrespective of whether the composites are based on magnesium or magnesium hydride, all of them show improved hydriding kinetics as compared to pure magnesium [53, 54], which is due to the presence of the intermetallic compound, a higher absorption capacity being attained after prolonged mechanical activation. The absorption capacity values achieved at different temperatures after 1 h hydriding are shown in Table 1. It is evident that these values are higher with the Mg-VTiFe samples, which is probably connected with the presence of

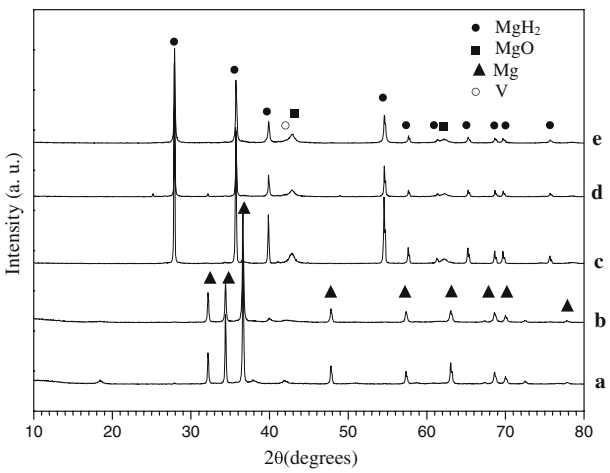

Fig. 1 X-ray diffraction patterns of: (a) 90 wt.% Mg–10 wt.% $V_{0.855}Ti_{0.095}Fe_{0.05}$ ball milled 1 h; (b) 90 wt.% Mg–10 wt.% $V_{0.855}Ti_{0.095}Fe_{0.05}$ ball milled 5 h; (c) synthesized MgH_2; (d) 90 wt.% MgH_2–10 wt.% $V_{0.855}Ti_{0.095}Fe_{0.05}$ ball milled 1 h; and (e) 90 wt.% MgH_2–10 wt.% $V_{0.855}Ti_{0.095}Fe_{0.05}$ ball milled 5 h

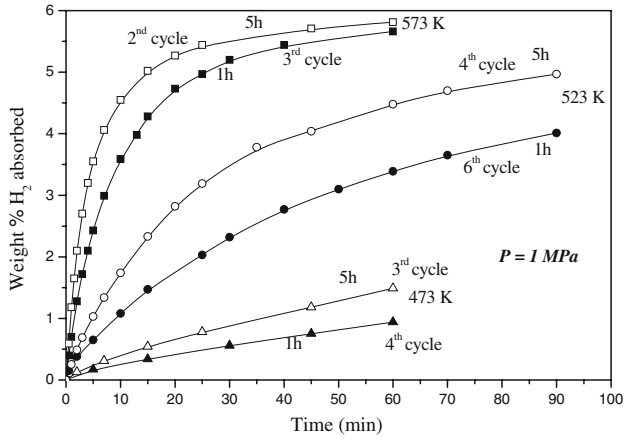

Fig. 2 Kinetic curves of hydriding of the composite 90 wt.% Mg–10 wt.% $V_{0.855}Ti_{0.095}Fe_{0.05}$ at different temperatures and a pressure of 1 MPa

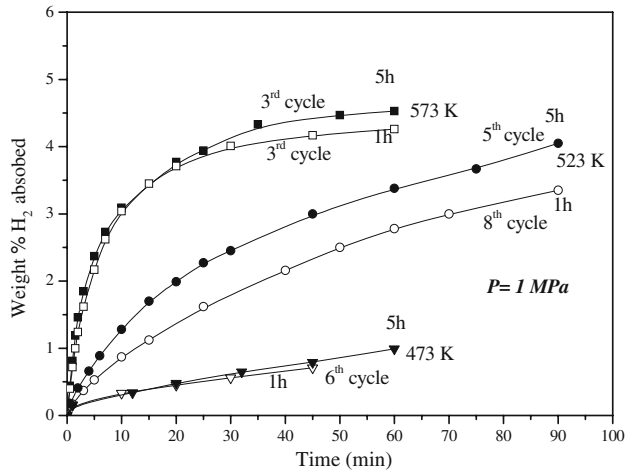

Fig. 3 Kinetic curves of hydriding of the composite 90 wt.% MgH_2–10 wt.% $V_{0.855}Ti_{0.095}Fe_{0.05}$ at different temperatures and a pressure of 1 MPa

Table 1 Absorption characteristics of the composites after 60 min hydriding at different temperatures and a pressure of 1 MPa

Composite	Ball milling duration (h)	Absorption capacity (wt.% H_2)		
		573 K	523 K	473 K
90% Mg–10% VTiFe[a]	1	5.66	4.01	0.94
90% Mg–10% VTiFe	5	5.81	4.97	1.49
90% MgH_2–10% VTiFe	1	4.74	3.35	0.86
90% MgH_2–10% VTiFe	5	4.46	3.38	0.56

[a] VTiFe = $V_{0.855}Ti_{0.095}Fe_{0.05}$

magnesium oxide in the composites MgH_2-VTiFe. The formation of a hydroxide layer on the surface of the air exposed samples is the main reason for the deteriorated hydriding/dehydriding properties of Mg_2Ni, as is shown by

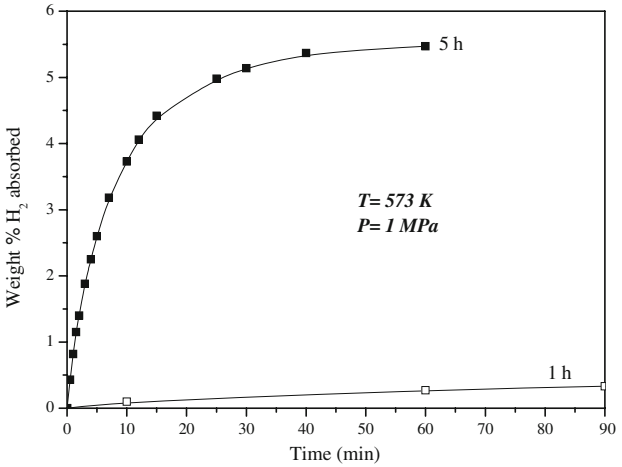

Fig. 4 First cycle of hydriding of the composite 90 wt.% Mg–10 wt.% $V_{0.855}Ti_{0.095}Fe_{0.05}$ at 573 K and a pressure of 1 MPa

Liu et al. [55]. The quantitative analysis was carried out with TOPAS V3 programme [52]. For the composites based on MgH_2, the theoretical absorption capacity will be lower by around 1.8 wt. %, because of the quantity of MgO in the starting MgH_2.

The kinetic curves of hydrogen absorption during the first cycle of hydriding of the composite Mg-VTiFe at 573 K (Fig. 4) show that after a prolonged milling in a planetary mill the composite needs no preliminary activation and reaches absorption capacity values close to the maximum one measured at this temperature already at the beginning of the hydriding process. The hydriding behaviors at 573 K of the four samples under consideration are compared in Fig. 5 where a more pronounced acceleration of the process is observed with the composite Mg-VTiFe mechanically activated for 5 h.

Figure 6 illustrates the kinetic curves of dehydriding at 623 K and $P = 0.15$ MPa for all the composites investigated. The curves almost overlap at the beginning of the desorption process, after which the desorption of hydrogen from the composites MgH_2-VTiFe is retarded as compared with that of composites Mg-VTiFe. A drastic decrease in amount of the desorbed hydrogen is, however, observed with all composites if desorption is carried out at the same pressure and the temperature is lowered to 573 K. Thus, the composite 90% Mg–10% VTiFe desorbs only 0.2% hydrogen in 1 h.

The catalytic effect of the additive may probably be attributed to the presence of iron clusters on the surface, this facilitating dissociative chemisorption of hydrogen. The presence of such clusters was established while measuring the magnetic characteristics of the intermetallic compound $V_{0.855}Ti_{0.095}Fe_{0.05}$ [50].

The calculated crystallite size of all composites varied between 49 and 101 nm. The corresponding values along

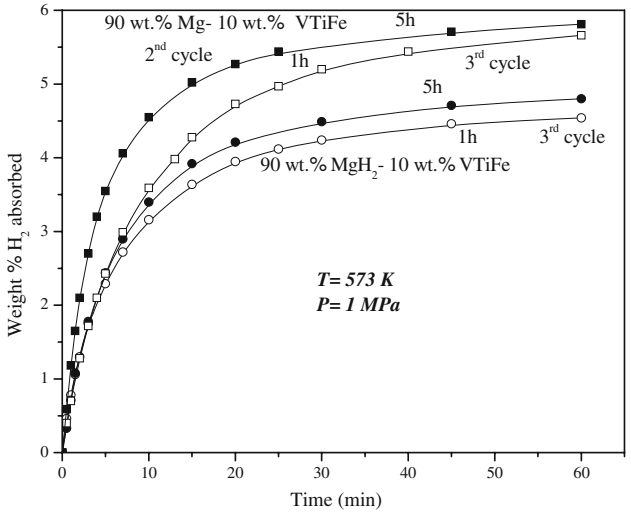

Fig. 5 Kinetic curves of hydriding of the composites investigated at 573 K and a pressure of 1 MPa

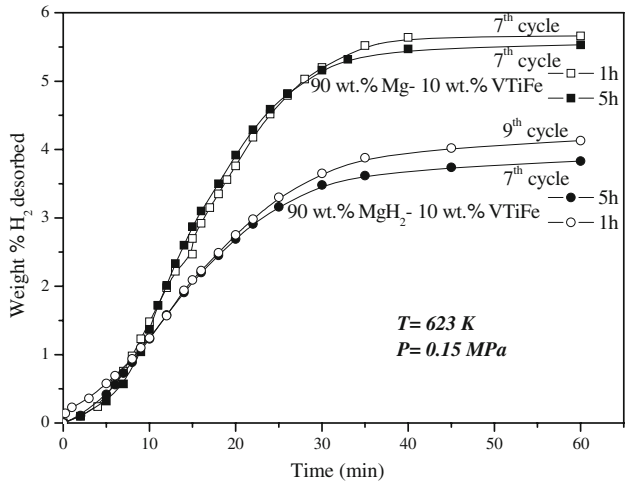

Fig. 6 Kinetic curves of dehydriding of the composites investigated at 623 K and a pressure of 0.15 MPa

with the BET values of the specific surface area of the samples are shown in Table 2.

From the data on the composite MgH_2-VTiFe it is evident that prolonging the duration of mechanical activation from 1 to 5 h is not associated with a noticeable increase in specific surface area. Simultaneously, the crystallite size shows a twofold decrease. There is a similar situation with the Mg-VTiFe composite. In the literature it is usually assumed [56] that the crystallite and particle sizes strongly affect the absorption characteristics of magnesium-based systems. According to Dornheim et al. [48], the effect of the crystallite size on the hydriding kinetics is more pronounced when the crystallites are bigger than 100 nm. In the studies of these authors and of many others, the duration of mechanical activation applied is of the order of tens

Table 2 Specific surface area and crystallite size values of the composites

Composite	Ball milling duration (h)	Specific surface area (m^2/g)		Initial crystallite size (nm)
		Initial	Hydrided	
90% MgH_2–10% VTiFe	1	15	19	101
90% MgH_2–10% VTiFe	5	16	–	49
90% Mg–10% VTiFe	1	4	9	81
90% Mg–10% VTiFe	5	5	–	55

or even hundreds of hours. In our case no drastic differences in behavior of the composites during hydriding–dehydriding should be expected because both the specific surface area (on which the particle size depends) and the crystallite size after 1 and 5 h of mechanical activation are of the same order of magnitude. Nevertheless, as is evident from the curve shapes in Figs. 2 and 3, the prolonged milling affects favorably the hydriding kinetics with both kinds of composites.

The shape of the absorption curves in Fig. 5 evidences a certain acceleration of the hydriding reaction for the composite 90 wt.% Mg–10 wt.% VTiFe ball milled for 5 h while the remaining three samples show almost the same hydriding rate. If, as already mentioned, the hydriding kinetics depend mainly on the particle size of the composite, i.e. on its specific surface area, the change of the latter with prolonging the duration of activation will be larger than is the case for the system 90 wt.% MgH_2–10 wt.% VTiFe, which would also explain the steeper hydriding curve of the composite 90 wt.% Mg–10 wt.% VTiFe.

On the other hand, hydrogen diffusion is correlated with the crystallite size and the facilitation of the diffusion in systems with smaller crystallites should be associated with an increase in absorption capacity. In this connection, due to the fact that the crystallite sizes of the composites under consideration show no substantial differences, their hydrogen absorption capacities are also close in value when taking into account that the samples of the type MgH_2-VTiFe contain magnesium oxide.

In Figs. 7 and 8, the X-ray diffraction patterns of hydrided/dehydrided magnesium and MgH_2-based composites ball milled under argon for 1 h are presented. The composites have been hydrided at 573 K and $P = 1$ MPa and dehydrided at 623 K under vacuum. Even after 90 min under vacuum at 623 K in the composite based on MgH_2, some hydride of magnesium is not decomposed. In the X-ray diffraction patterns of hydrided and dehydrided 90 wt.% MgH_2–10 wt.% VTiFe ball milled for 1 h (Fig. 7), the peaks of MgO are more visible and with a higher intensity. This can be explained by a larger specific

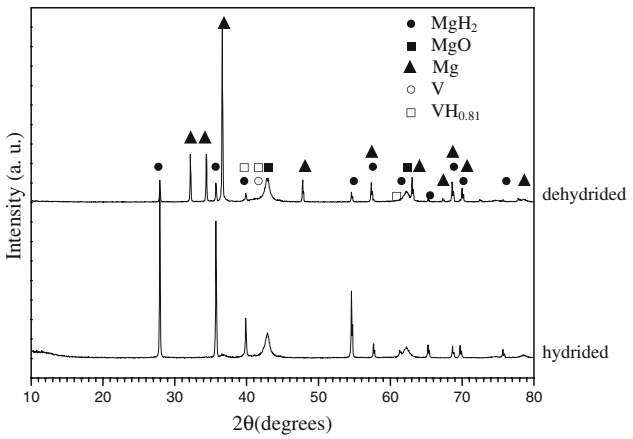

Fig. 7 X-ray diffraction patterns of the composite 90 wt.% MgH_2–10 wt.% $V_{0.855}Ti_{0.095}Fe_{0.05}$ ball milled 1 h after hydriding and dehydriding

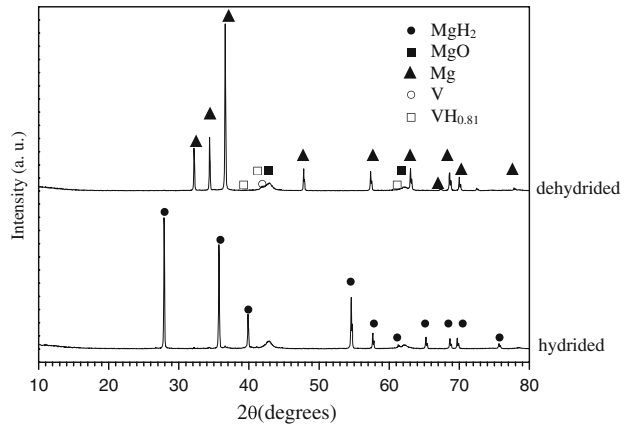

Fig. 8 X-ray diffraction patterns of the composite 90 wt.% Mg–10 wt.% $V_{0.855}Ti_{0.095}Fe_{0.05}$ ball milled 1 h after hydriding and dehydriding

surface area and because of that these composites are more sensitive to air exposure.

On the basis of their absorption–desorption performances, the composites studied follow the sequence:

90 wt.% Mg–10 wt.% VTiFe (5 h) > 90 wt.% MgH_2–10 wt.% VTiFe (5 h) > 90 wt.% Mg-10 wt.% VTiFe (1 h) > 90 wt.% MgH_2–10 wt.% VTiFe (1 h).

Conclusion

The results obtained on the absorption–desorption characteristics of the composites 90 wt.% Mg (MgH_2)–10 wt.% $V_{0.855}Ti_{0.095}Fe_{0.05}$ demonstrate the positive effect of the intermetallic compound additive on the hydriding of magnesium. The composites investigated have a high absorption capacity below 573 K and improved hydriding–dehydriding kinetics. Due to the fact that with the duration of mechanical activation chosen no significant change in particle size occurs, the hydriding kinetics show no substantial change. The presence of magnesium oxide in the composites based on magnesium hydride determines their lower absorption capacity as compared to magnesium-based composites.

Acknowledgements The financial support of the National Fund of Scientific Investigations of Bulgaria under contract No X-1407/2004 is highly appreciated.

References

1. Ivanov EY, Konstanchuk IG, Stepanov AA, Boldyrev VV (1986) Dokl Akad Nauk SSSR 286:385
2. Konstanchuk IG, Ivanov EY, Pezat M, Darriet B, Hagenmuller P (1987) J Less-Common Met 131:181
3. Bobet J-L, Pechev S, Chevalier B, Darriet B (1999) J Mater Chem 9:315
4. Khrussanova M, Grigorova E, Mitov I, Radev D, Peshev P (2001) J Alloys Compd 327:230
5. Bobet J-L, Akiba E, Darriet B (2001) Int J Hydrogen Energy 26:493
6. Gennari FC, Castro FJ, Urretavizcaya G, Meyer G (2002) J Alloys Compd 334:277
7. Bououdina M, Guo ZX (2002) J Alloys Compd 335:222
8. Song MY (2003) Int J Hydrogen Energy 28:403
9. Liang G, Schulz R (2004) J Mater Sci 39:1557. doi:10.1023/B:JMSC.0000016151.51658.08
10. De Castro JFR, Santos SF, Costa ALM, Yavari AR, Botta WJF, Ishikawa TT (2004) J Alloys Compd 376:251
11. Belouis LEA, Honnor P, Hall PJ, Morris S, Dodd SB (2006) J Mater Sci 41:6403. doi:10.1007/s10853-006-0732-1
12. Czujko T, Varin RA, Chiu Ch Wronski Z (2006) J Alloys Compd 414:240
13. Hashimoto H, Sun ZM (2006) J Alloys Compd 417:203
14. Khrussanova M, Terzieva M, Peshev P, Konstanchuk IG, Ivanov EY (1989) Z Phys Chem (NF) 164:1261
15. Khrussanova M, Terzieva M, Peshev P, Konstanchuk I, Ivanov E (1991) Mater Res Bull 26:561
16. Wang P, Wang AM, Zhang HF, Ding BZ, Hu ZQ (2000) J Alloys Compd 313:218
17. Song MY, Bobet J-L, Darriet B (2003) J Alloys Compd 340:256
18. Bobet J-L, Desmoulins-Krawiec S, Grigorova E, Cansell F, Chevalier B (2003) J Alloys Compd 351:217
19. Castro FJ, Bobet J-L (2004) J Alloys Compd 366:303
20. Song MY, Kwon IH, Bae J-S (2005) Int J Hydrogen Energy 30:1107
21. Huang ZG, Guo ZP, Calka A, Wexler D, Lukey C, Liu HK (2006) J Alloys Compd 422:299
22. Vijay R, Sundaresan R, Maiya MP, Srinivasa Murthy S (2006) J Alloys Compd 424:289
23. Dolci F, Di Chio M, Baricco M (2007) J Mater Sci 42:7180. doi:10.1007/s10853-007-1567-0
24. Terzieva M, Khrussanova M, Peshev P, Radev D (1995) Int J Hydrogen Energy 20:53
25. Guoxian L, Erde W, Shoushi F (1995) J Alloys Compd 223:111
26. Terzieva M, Khrussanova M, Peshev P (1998) J Alloys Compd 267:235
27. Liang G, Boily S, Huot J, Van Neste A, Schulz R (1998) J Alloys Compd 268:302
28. Sai Raman SS, Davidson DJ, Srivastava ON (1999) J Alloys Compd 292:202

29. Yang J, Ciureanu M, Roberge R (2000) Mater Lett 43:234
30. Wang P, Zhang HF, Ding BZ, Hu ZQ (2001) Acta Mater 49:921
31. Wang P, Wang AM, Ding BZ, Hu ZQ (2002) J Alloys Compd 334:243
32. Bobet J-L, Grigorova E, Khrussanova M, Khristov M, Radev D, Peshev P (2002) J Alloys Compd 345:280
33. Hu YQ, Zhang HF, Wang AM, Ding BZ, Hu ZQ (2003) J Alloys Compd 354:296
34. Khrussanova M, Grigorova E, Bobet J-L, Khristov M, Peshev P (2004) J Alloys Compd 365:308
35. Hu YQ, Yan C, Zhang HF, Ye L, Hu ZQ (2004) J Alloys Compd 375:265
36. Kondo T, Shindo K, Arakawa M, Sakurai Y (2004) J Alloys Compd 375:283
37. Vijay R, Sundaresan R, Maiya MP, Srivansa Murthy S, Fu Y, Klein H-P, Groll M (2004) J Alloys Compd 384:283
38. Gu H, Zhu Y, Li L (2006) J Alloys Compd 424:382
39. Khrussanova M, Mandzhukova TS, Grigorova E, Khristov M, Peshev P (2007) J Mater Sci 42:3338. doi:10.1007/s10853-006-0586-6
40. Liu X, Huang Z, Jiang L, Wang S (2007) Int J Hydrogen Energy 32:965
41. Ivanov E, Konstanchuk I, Bokhonov B, Boldyrev V (2003) J Alloys Compd 359:320
42. Bouaricha S, Dodelet JP, Guay D, Huot J, Schulz R (2001) J Alloys Compd 325:245
43. Imamura H, Tabata S, Shigetomi N, Takesue Y, Sakata Y (2002) J Alloys Compd 330–332:579
44. Imamura H, Kusuhara M, Minami S, Matsumoto M, Masanari K, Sakata Y, Itoh K, Fukunaga T (2003) Acta Mater 51:6407
45. Bobet J-L, Grigorova E, Khrussanova M, Khristov M, Stefanov P, Peshev P, Radev D (2004) J Alloys Compd 366:298
46. Liang G, Huot J, Boily S, Van Neste A, Schulz R (1999) J Alloys Compd 291:295
47. Huot J, Liang G, Schulz R (2001) Appl Phys A 72:187
48. Dornheim M, Eigen N, Barkhordarian G, Klassen T, Bormann R (2006) Adv Eng Mater 8:377
49. Dornheim M, Doppiu S, Barkhordarian G, Boesenberg U, Klassen T, Gutfleisch O, Bormann R (2007) Scripta Mater 56:841
50. Khrussanova M, Peshev P, Darriet B, Petrova S (1992) Mater Res Bull 27:611
51. Tanguy B, Soubeyroux J-L, Pezat M, Portier J, Hagenmuller P (1976) Mater Res Bull 11:1441
52. Topas V3, General profile and structure analysis software for powder diffraction data, Brucker AXS, Karlsruhe, Germany (2006)
53. Grigorova E, Khristov M, Khrussanova M, Bobet JL, Peshev P (2005) Int J Hydrogen Energy 30:1099
54. Khrussanova M, Grigorova E, Mandzhukova TS, Khristov M, Bobet JL, Peshev P (2007) Bulgarian Chem Commun 39:123
55. Liu D, Zhu Y, Li L (2007) J Mater Sci 42:9725. doi:10.1007/s10853-007-2037-4
56. Zaluska A, Zaluski L, Ström-Olsen JO (1999) J Alloys Compd 288:217